Chapter 8

The Strain Energy Release Rate for Stack of Coated Conductors with Interface Crack in Perpendicular Magnetic Field

Meng Zhao, Huadong Yong and Youhe Zhou

Additional information is available at the end of the chapter

http://dx.doi.org/10.5772/64006

Abstract

Due to the ability of transporting huge current in the stack of high-temperature superconducting conductors, the electromagnetic body force generated by the interaction of magnetic field and current may affect the mechanical stability of structure. In this paper, the fracture behavior of the stack of coated conductors which contains an interface crack is studied for increasing field and decreasing field. The body forces are obtained with variational formulation for the Bean's critical state model. Based on the virtual crack closure technique (VCCT), the strain energy release rate of the stack of coated conductors with an interface crack is determined. The strain energy release rates are compared for different crack positions, crack lengths, magnetic fields and the thicknesses of substrate, respectively. These results may be useful for the practical application.

Keywords: strain energy release rate, stacked conductors, interface crack, magnetic field, superconductor

1. Introduction

Due to the ability of transporting high critical current density and trapping magnetic field, high-temperature superconductors have been expected to be used in the transmission cables, transformers, motors and maglev system [1–5]. A typical application is the stack of high-temperature superconductor coated tapes for power engineering [6]. However, the application of tape is limited for the reason that the superconductor is a brittle material, which cannot withstand large mechanical loadings [7, 8]. Meanwhile, the manufacturing process is complex

for high-temperature superconductor. Thus, the cavity and microcracks are inevitable in superconductor [9, 10]. The electromagnetic body force induced by the interaction of electromagnetic field may result in the extension of crack in superconductor under high magnetic fields, which will finally give rise to the fracture of superconductor [11]. Cracking can reduce the critical current density of superconductor and mechanical stability [12]. Recently, significant efforts have been made to study the mechanical behavior of the superconductors with the development of critical current density.

Since the electromagnetic behavior in superconductor is complex, several different theoretical models were presented to describe the constitutive relation, such as Bean model, Kim model and E-J relation [13–15]. In recent years, the relationships between mechanical response and magnetic field have been concerned [16, 17]. The general procedure is that the current and magnetic field distributions are obtained based on the constitutive model. After deriving the electromagnetic body force, we will find the mechanical characteristics of superconductor. The superconductor will undergo mechanical deformation in magnetic field which is regarded as magnetostriction. The magnetostriction is dependent on the amplitude of magnetic field and critical state model [16, 17]. For the superconductors during the magnetization, the body force induced by the flux pinning evolves from initially compressive to tensile as the external field changes from increasing to decreasing. It was pointed out that the stress and strain induced by flux pinning show obvious irreversible behavior. In other words, the stresses are different for increasing field and decreasing field cases [18–20]. Moreover, two different cooling processes (zero field cooling and field cooling) are discussed. The quantitative analysis on the magneto-elastic problems in bulks and strips was made for different critical state models, such as the Bean model and Kim model [18–31]. For superconducting strip with transport current, the magnetostriction curve is not a closed loop [32]. The stress and magnetostriction in many complex structures also have attracted many attentions [33–37].

The crack problem is another challenge for the superconductors because the electromagnetic body force and thermal stress are important driving forces for crack growth. During the cycles of the applied magnetic field, the tensile and compressive stress will be generated alternately and cracking of superconductor usually occurs as the field is decreased to zero [38]. This is because the crack is prone to advance under the tensile stress. The linear elastic fracture theory was widely used to investigate the fractures behaviors of the thin film and bulk superconductors [39–47]. The collinear cracks, transverse crack and crack-inclusion problems in superconductors were also studied recently [48–50]. Superconductors are usually metal composites which consist of several components. Then, the crack problems in inhomogeneous superconductors were studied extensively [51–57]. Recently, the dynamic fracture behaviors in superconductors were analyzed with the finite element method [58].

Compared to the bulk superconductor, coated conductors have better mechanical strength [59]. As is known to us, the coated conductor structure is made up of several layers deposited onto the substrate. In the coated conductor structure, the interface crack may be generated by lattice mismatch, thermal expansion and chemical reactions during the deposition progress of the coated structure [60]. The delamination of superconducting layer is easy to take place at the interface between dissimilar materials [61]. Unlike the internal or edge crack problems, the

http://dx.doi.org/10.5772/64006

compressive stress can also lead to the propagation of interface crack [62]. Thus, it is necessary to analyze the fracture behavior of interface crack to predict the mechanical instability in the coated conductor structure.

The fracture behavior of interface crack between superconducting film or tape and substrate was studied in magnetic field or with transport current [62–64]. However, there are few works on the crack problem in stack of conductors. In this paper, we consider the interface crack in the stack of high-temperature coated tapes. The effect of copper and substrate on the shielding current and magnetic field distributions in the superconducting layer is neglected. Based on the simplified geometrical and material assumptions, linear elastic equation is used. We carry out an in-depth investigation on the strain energy release rate for interface crack in different magnetic fields, crack lengths, substrate thicknesses with virtual crack closure technique (VCCT). The results may provide guidance for the design of stack of coated conductors.

This paper is organized as follows. In Section 2, we introduce VCCT to calculate the strain energy rate at the crack tip. Section 3 computes a bimaterial plate with a central interface crack to verify the accuracy of VCCT. In Section 4, we discuss the body force distribution in superconducting tape. In Section 5, the interface crack in stack of tapes is analyzed under perpendicular magnetic field. In Section 6, we draw a conclusion from the above work.

2. Strain energy release rate of interface crack using VCCT

In this section, we will first verify the accuracy of the numerical computation. Here, we only consider the linear elastic fracture behavior. For the interface crack problem, the stress intensity factor or strain energy release rate can be determined with the virtual crack closure technique (VCCT). VCCT is a well-established method for computing the crack problem [65], which was proposed by Rybicki and Kanninen for two-dimensional problems [66].

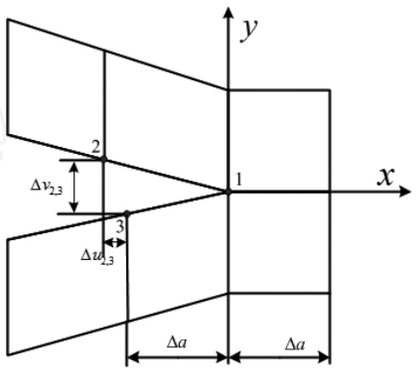

Figure 1. Calculating model of the strain energy release rate using VCCT.

Figure 1 shows the mesh model for computing the strain energy release rate with VCCT, where u and v stand for the displacement along x and y directions, respectively. Each mesh is a square and Δa is the side width. On the basis of assumption given in reference [66], we

define the opening displacement behind the tip of virtual crack ($\Delta v_{2,3}$ and $\Delta u_{2,3}$) as the actual crack opening displacement for determining strain energy release rate with VCCT. The strain energy release rate represents the change of elastic strain energy per unit area of crack extension [67]. Then, the strain energy release rates for different fracture modes can be expressed as follows:

$$G_{\mathrm{I}} = \frac{F_y \Delta v_{2,3}}{2B\Delta a},\ G_{\mathrm{II}} = \frac{F_x \Delta u_{2,3}}{2B\Delta a} \tag{1}$$

$$G = G_{\mathrm{I}} + G_{\mathrm{II}} \tag{2}$$

where F_x and F_y are the nodal forces and B is the thickness of the body with crack. VCCT is an effective method which does not need integration and it is insensitive to mesh.

3. Verification of numerical results

In order to verify the simulation results, we study the fracture behavior for bimaterial plate with an interface crack, as shown in **Figure 2**. It is well known that for the interface crack, there is the coupling between the tensile fracture mode and shear fracture mode even for mode I loadings. In addition, the oscillation of stress singularity will occur at the crack tip [65]. In this model, the interface crack is located in the center of the bimaterial plate and a uniform tension load σ_0 is applied on the top and bottom edges of the plate. The parameters used for numerical analysis are as follows [68]: $2w$ = 100 mm, $2l$ = 200 mm, a/w = 0.4, $E_1 = 2.058 \times 10^5$ MPa, $\frac{E_1}{E_2} = 1 \sim 100$, $v_1 = v_2 = 0.3$, $\sigma_0 = 9.8$ MPa.

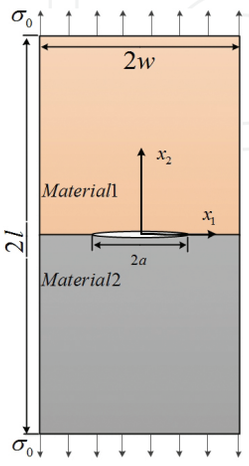

Figure 2. A finite bimaterial plate with interface crack under a uniform tension.

http://dx.doi.org/10.5772/64006

We use finite element software Abaqus to solve the interface crack problem. A 4-node bilinear plane stress quad-dominated structured element is used and mesh width is given as $\Delta a = 1$mm. It is convenient for us to use VCCT to compute the strain energy release rate. For the sake of comparing our results with those of Yu et al. [69], Nagashima et al. [70], Miyazaki et al. [71], we use the formulation proposed by Suo and Hutchinson [72]. For bimaterial interface crack problem, the relation between stress intensity factor and strain energy release rate is as follows [72]

$$G = \frac{c_1 + c_2}{16\cosh^2 \pi\varepsilon}|K|^2 \tag{3}$$

where subscripts 1 and 2 represent the material 1 and material 2, respectively, and

$$K^2 = K_1^2 + K_2^2 \tag{4}$$

$$c_1 = \frac{\kappa_1 + 1}{\mu_1},\ c_2 = \frac{\kappa_2 + 1}{\mu_2} \tag{5}$$

$$\varepsilon = \frac{1}{2\pi}\ln\frac{1-\beta}{1+\beta},\ \kappa = (3-\upsilon)/(1+\upsilon) \tag{6}$$

$$\beta = \frac{\mu_1(\kappa_2 - 1) - \mu_2(\kappa_1 - 1)}{\mu_1(\kappa_2 + 1) + \mu_2(\kappa_1 + 1)} \tag{7}$$

in which β is the parameter proposed by Dundurs to describe the mismatch of material 1 and material 2 [73], and μ is the shear modulus.

Table 1 shows the comparison of strain energy release rates for present work and the results given by others when $a/w = 0.4$. These results show that there is little difference between our work using VCCT and other methods. The difference is smaller than 1% and this verifies the accuracy of the numerical method.

E1/E2	Yu	Nagashima	Miyazaki	This work
1	0.0361	0.0361	0.0362	0.0358
2	0.0531	0.0529	0.0231	0.0526
3	0.0688	0.0685	0.0690	0.0683
4	0.0841	0.0835	0.0843	0.0834
10	0.1725	0.1699	0.1727	0.1711
100	1.4652	1.4264	1.4642	1.4529

Table 1. Comparison of the strain energy release rate G (N/mm).

4. Body force distribution in tape under magnetic field

Next, we turn our attention to the body force distributions in superconducting tape. **Figure 3** shows the configuration of the stack of superconducting conductors. The conductors consist of three tapes and these tapes are separated by the insulation layers (green). Generally, the superconducting layer (black) is attached to the substrate in each tape. In addition, copper layer is deposited on the superconducting layer which can also transport current. The thicknesses of the insulation layer, copper layer, superconducting layer and substrate are h_{Ins} = 25 μm, h_{Cop} = 40 μm, h_{SC} = 1 μm, h_{Sub} = 50 μm, respectively [74]. Then, the total thickness of stacked conductors is h = 373 μm and the width is 200 μm. The mechanical behavior is based on the electromagnetic body force and we will first calculate the field and current distributions. For simplicity, we use the Bean's critical state model, i.e., the critical current density is a constant which is independent of the magnetic field.

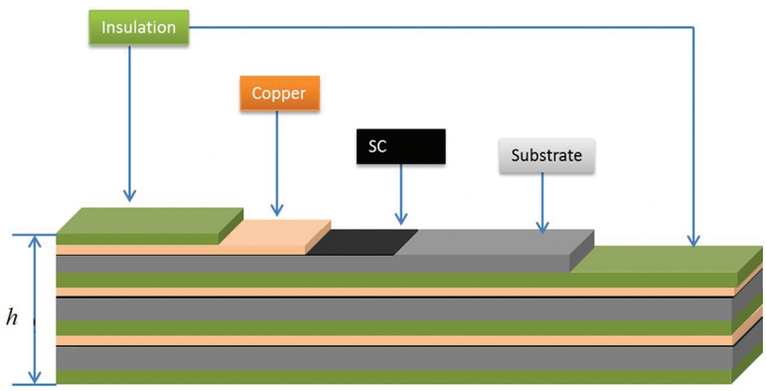

Figure 3. The configuration of the stack of superconducting conductors.

The distributions of shielding current are plotted in **Figure 4**. As the conductor is under magnetic field, the current will be induced to shield the external field. From **Figure 4 (a)**, we can find that the tape is divided into two parts and the current direction is opposite in two parts for increasing field case. As the external field is decreased, the shielding current will redistribute. The conductor can be divided into four parts for decreasing field case. However, it is interesting to see that the direction of shielding current is antisymmetric.

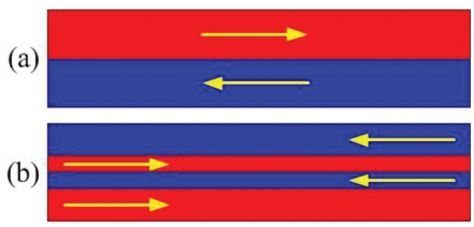

Figure 4. The current distribution in superconducting layer under magnetic field. (a) Increasing field case and (b) decreasing field case.

http://dx.doi.org/10.5772/64006

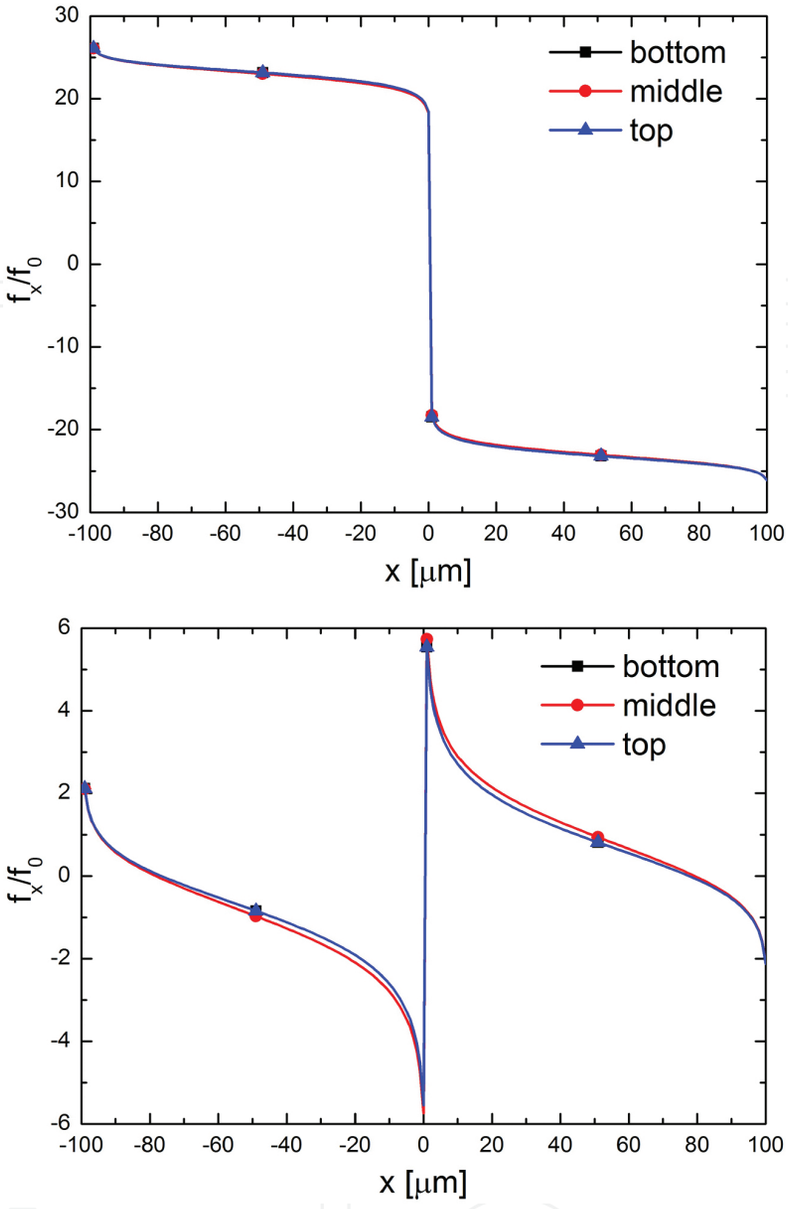

Figure 5. The distributions of body force along x direction. The magnetic field is increased from zero to B_e (upper). The field is decreased from B_e to zero (lower).

Using the variational formulation derived by Prigozhin [75], the electromagnetic responses of superconducting layer are obtained in the external field. The body force **f = j**×B can be determined with the flux density and current. **Figures 5** and **6** present the body forces f_x and f_y per unit volume for various stages of magnetization process. It is obvious that the body forces along x direction are very close for the bottom, middle and top layers. Moreover, the value of f_x for the increasing field is larger than that for decreasing field. The body force f_y is much smaller than f_x. This is due to the reason that the magnetic field is mainly along y direction. Thus, it can be expected that shear loading is important than the tensile loading. As external field B_e is larger than the full penetration field, the value of f_y for increasing and decreasing field is also very close.

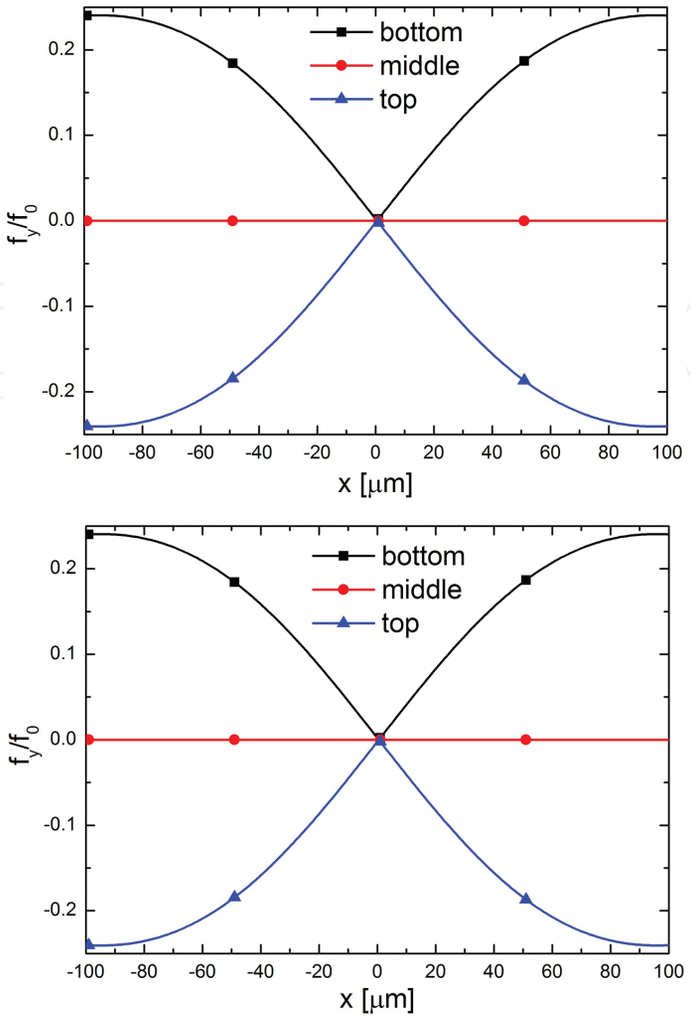

Figure 6. The distributions of body force along y direction. The magnetic field is increased from zero to B_e (upper). The field is decreased from B_e to zero (lower).

5. Interface crack problem for the stacked conductors structure

The structure of the stack of high-temperature superconducting conductors in perpendicular magnetic field is shown in **Figure 7**. The lower insulation layer which is located at the bottom is fixed. That is to say that the displacements of x and y directions at the bottom of conductors are zero. The stacked conductors consist of three superconducting tapes. The central interface crack is located between the superconducting layer and substrate, and is assumed to be through the length of conductor.

Although copper is an elasto-plastic material, we neglect the plastic deformation. Thus, the focus will be on the linear fracture mechanics problem. All constituent materials are isotropic, linearly elastic and homogeneous. The effects of copper and substrate on the distributions of magnetic field and current density in the superconductor layer can be ignored and the stack

http://dx.doi.org/10.5772/64006

of superconducting conductors is placed in a magnetic field B parallel to the y direction. Since the interface crack is parallel to the direction of current flowing, the crack will not disturb the current density and field distributions. Moreover, the width of the stacked conductors is much smaller than the length of the tape along z direction. For the 2D dimensional analysis, a plane strain condition can be assumed.

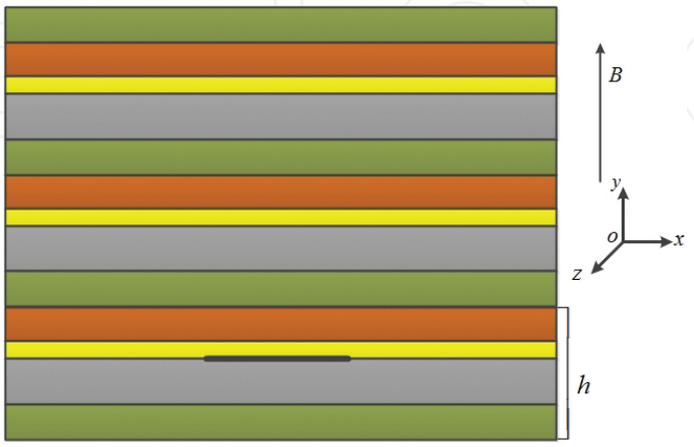

Figure 7. Schematic drawing of the stacked conductors with an interface crack in the perpendicular magnetic field.

During the following simulations, the used parameters are given as follows. We assume that the current density j is no larger than the critical current value $j_c = 3\times10^4$ A/mm^2. Besides, the applied maximum field is equal to $B_e = 8\mu_0 j_c t$, t is the thickness of the total superconducting layers and μ_0 is permeability in vacuum. The strain energy release is normalized by $G_0 = \frac{(1-\nu^2)\pi a}{E_{sc}}\left(\frac{\mu_0 j_c^2 tw}{\pi}\right)^2$.

	***E*(MPa)**	**Poisson's ratio**
Copper	117×10^3	0.35
YBCO	178×10^3	0.3
Hastelloy	200×10^3	0.3
Insulation	3.5×10^3	0.3

Table 2. Parameters of the materials of the coated tapes [74].

We consider the magnetization process in which the field is increased from zero to maximum and subsequently decreased to zero. As discussed earlier, the body force direction will change for increasing field and decreasing field. Since the total strain energy release rate for increasing field is larger, we mainly discuss the increasing field case. We can assume $G_I = 0$ when the interface crack is closed [62]. For the sake of simplicity, the contact and friction effects between crack surfaces are not considered. The parameters used are given in **Table 2**.

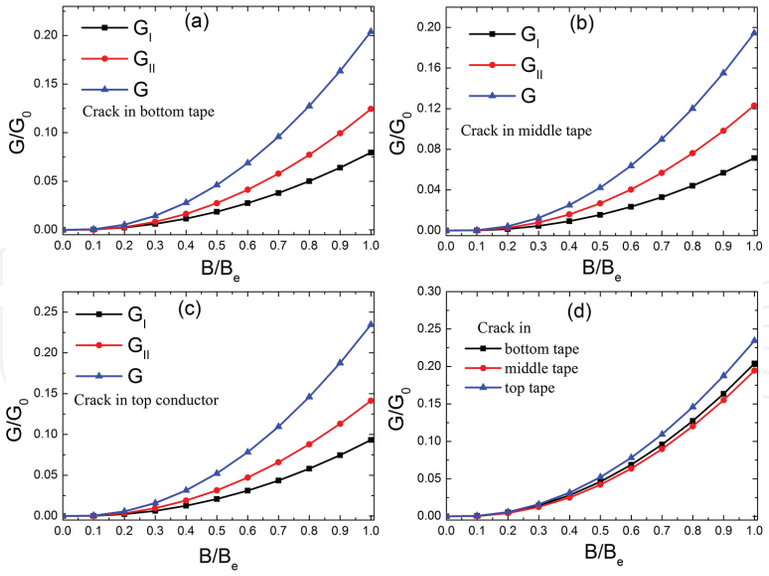

Figure 8. The variation of strain energy release rates with magnetic field as the interface crack is in (a) top tape, (b) middle tape and (c) top tape. The strain energy release rates are compared in (d).

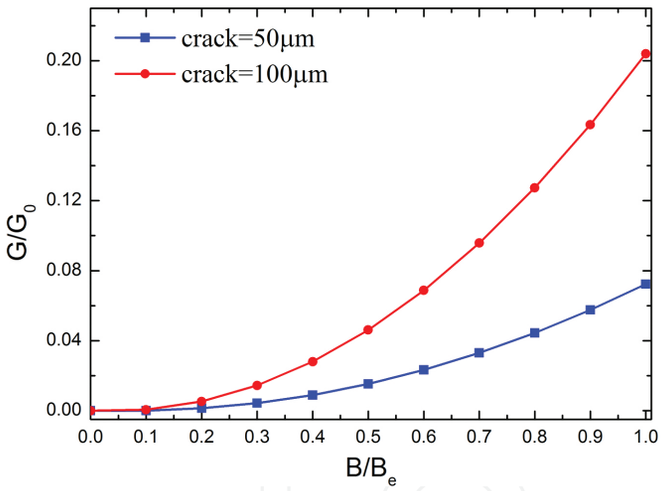

Figure 9. The strain energy release rates for the crack lengths of 50 μm and 100 μm during increasing magnetic field.

Next, we will calculate the strain energy release rates for the stacked conductors with the interface crack. **Figure 8(a)–(c)** shows the variation of strain energy release rate with the magnetic field, i.e., the field is increased from zero to maximum. The central interface crack is located at the bottom, middle or top tape. It can be found that all the strain energy release rates increase with the increasing field. Although the body force is compressive for increasing field case, G_I is smaller than G_{II} and this trend is similar to the results given in reference [62]. The strain energy release rates with interface crack in different tapes are compared in **Figure 8(d)**. It can be found that the strain energy release rate reaches the largest value as the interface crack is in the top tape during the increasing of field, while the value is the lowest as the crack is in the middle tape. We can draw a conclusion that the central interface crack in the top tape is

http://dx.doi.org/10.5772/64006

most dangerous during an increasing magnetic field. This may be due to the reason that the penetration field is largest in the top tape. In **Figure 9**, it is to be noted that the strain energy release rate for the crack length of 100 μm is always larger than that of 50 μm when the magnetic field rises. However, since the shielding current reverses, the trend of strain energy release rate becomes complicated for decreasing field case, as shown in **Figure 10**. At the beginning of the decreasing field, both the strain energy release rates for the crack lengths of 100 μm and 50 μm reduce. It is obvious that the reduction for longer crack length is faster. With the decreasing external field, the strain energy release rate reaches the local minimum and begins to increase. The longer crack firstly reaches the local minimum at B/B_e = 0.88. Finally, the strain energy release rate will decrease again, and the value is very close to zero as external field vanishes. Comparing the values for increasing field and decreasing field (see **Figure 11**), we can find that the strain energy release rate is larger for increasing field case. Thus, the highest possibility of cracking may happen during the increasing field, which is opposite to the bulk superconductor.

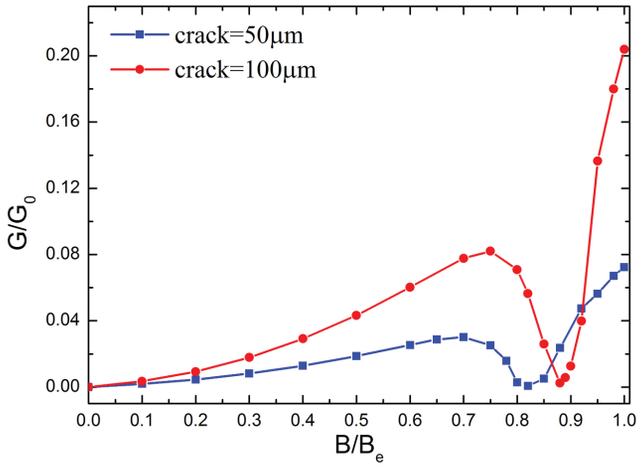

Figure 10. The strain energy release rates for the crack lengths of 50 μm and 100 μm during decreasing magnetic field.

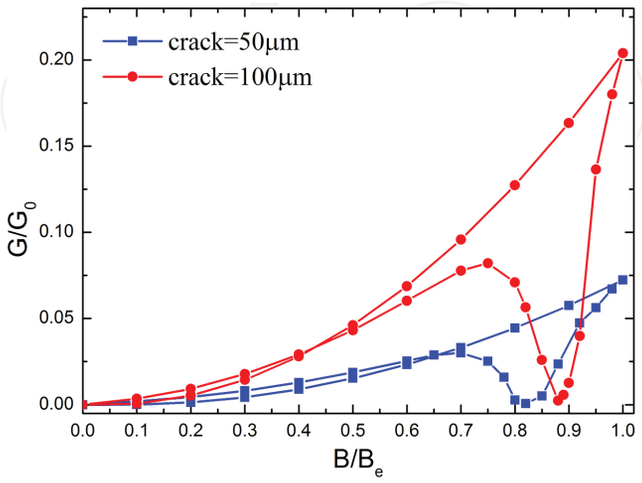

Figure 11. The comparison of strain energy release rates for increasing field and decreasing field.

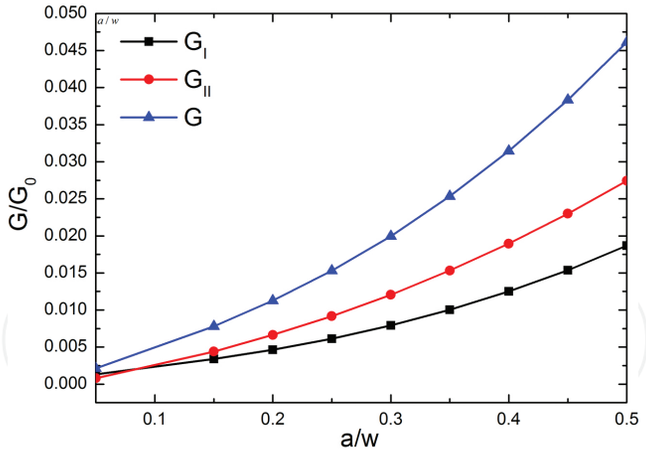

Figure 12. The change of strain energy release rate with the crack length and as the field is increased from zero to $0.5B_e$.

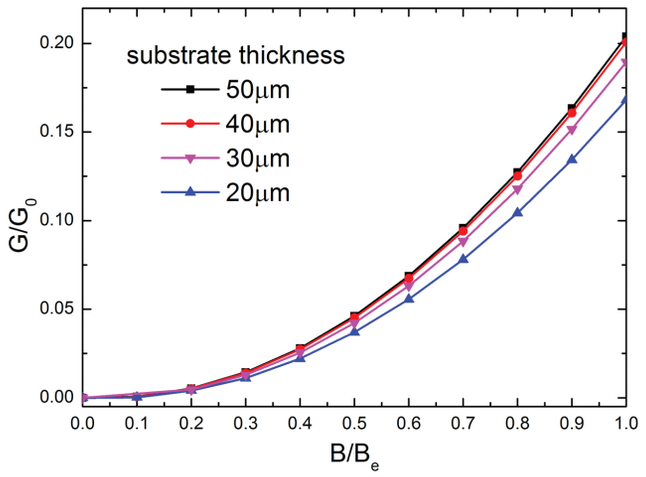

Figure 13. The strain energy release rates with different thicknesses of substrate.

For the central interface crack problem, it can be expected that the strain energy release rate increases with the length of the crack for a fixed magnetic field, as shown in **Figure 12**. The effect of substrate thickness on the strain energy release rate during increasing field is presented in **Figure 13**. One can find that with the increase of substrate thickness from 20 μm to 50 μm, the strain energy release rate also rises. In addition, the increasing strain energy release rate is more obvious in high field. However, the difference is very small as the thickness of substrate is larger than 40 μm. Thus, it is reasonable to reduce the thickness of substrate to improve the mechanical stability of stacked conductors structure.

6. Conclusions

In this paper, we considered the interface crack in the stack of high-temperature superconductor coated conductors with VCCT. A simple interfacial crack problem in bimaterial was

http://dx.doi.org/10.5772/64006

calculated to verify the accuracy of numerical method. On the basis of the linear elastic fracture theory, the strain energy release rates for the stack of coated conductors with interface crack were presented for different magnetic fields, crack lengths, substrate thicknesses. The strain energy release rate increases monotonically with the increasing external field. However, the trend for decreasing field case is not monotonic. When the interface crack is located in the top tape, the strain energy release rate is the largest. In addition, the thickness of hastelloy substrate also has an effect on the strain energy release rate, and larger thickness leads to the higher energy release rate. When the thickness of the substrate is larger than 40μm, the effect of thickness becomes negligible. This study may provide a better understanding on the mechanical instability of the stack of coated conductor structure during the magnetization process.

Acknowledgements

We acknowledge the support from the Innovative Research Group of the National Natural Science Foundation of China (11421062), National Natural Science Foundation of China (Nos. 11202087 and 11472120), the National Key Project of Magneto-Constrained Fusion Energy Development Program (No. 2013GB110002), the National Key Project of Scientific Instrument and Equipment Development (No. 11327802) and New Century Excellent Talents in University of Ministry of Education of China (NCET-13-0266).

Author details

Meng Zhao, Huadong Yong* and Youhe Zhou

*Address all correspondence to: yonghd@lzu.edu.cn

Key Laboratory of Mechanics on Environment and Disaster in Western China, The Ministry of Education of China, Department of Mechanics and Engineering Sciences, College of Civil Engineering and Mechanics, Lanzhou University, Lanzhou, Gansu, PR China

References

[1] Bohno T, Tomioka A, Imaizumi M, et al. Development of 66 kV/6.9 kV 2 MVA prototype HTS power transformer. Physica C: Superconductivity and its Applications, 2005, 426–431: 1402–1407. DOI: 10.1016/j.physc.2005.03.080

[2] Igarashi M, Nakao H, Terai M, et al. Persistent current HTS magnet cooled by cryocooler (1)—project overview. IEEE Transactions on Applied Superconductivity, 2005, 15(2): 1469–1472. DOI: 10.1109/TASC.2005.849130

[3] Wiezoreck J, Schmidt F, Nick W, et al. Development of HTS power transmission cables. IEEE Transactions on Applied Superconductivity, 1999, 9(2): 406–411. DOI: 10.1109/77.783321

[4] Choi S, Kiyoshi T, Hahn S Y, et al. Stress analysis of a high temperature superconductor coil wound with Bi-2223/Ag tapes for high field HTS/LTS NMR magnet application. IEEE Transactions on Applied Superconductivity, 2009, 19(3): 2237–2240. DOI: 10.1109/TASC.2009.2018071

[5] Song H H, Brownsey P, Zhang Y F, et al. 2G HTS coil technology development at SuperPower. IEEE Transactions on Applied Superconductivity, 2013, 23(3): 4600806. DOI: 10.1109/TASC.2012.2233837

[6] Augieri A, De Marzi G, Celentano G, et al. Electrical characterization of ENEA high temperature superconducting cable. IEEE Transactions on Applied Superconductivity, 2015, 25(3): 1–4. DOI: 10.1109/TASC.2014.2364391

[7] Durrell J H, Dennis A R, Jaroszynski J, et al. A trapped field of 17.6 T in melt-processed, bulk Gd-Ba-Cu-O reinforced with shrink-fit steel. Superconductor Science and Technology, 2014, 27(8): 082001. DOI: 10.1088/0953-2048/27/8/082001

[8] Gruss S, Fuchs G, Krabbes G, et al. Superconducting bulk magnets: very high trapped fields and cracking. Applied Physics Letters, 2001, 79(19): 3131–3133. DOI: 10.1063/1.1413502

[9] Diko P, Krabbes G. Macro-cracking in melt-grown Y-Ba-Cu-O superconductor induced by surface oxygenation. Superconductor Science and Technology, 2002, 16(1): 90. DOI: 10.1088/0953-2048/16/1/316

[10] Diko P, Krabbes G. Formation of c-macrocracks during oxygenation of TSMG YBa2Cu3O7/Y2BaCuO5 single-grain superconductors. Physica C: Superconductivity, 2003, 399(3): 151–157. DOI: 10.1016/S0921-4534(03)01305-4

[11] Ren Y, Weinstein R, Liu J, et al. Damage caused by magnetic pressure at high trapped field in quasi-permanent magnets composed of melt-textured Y-Ba-Cu-O superconductor. Physica C: Superconductivity, 1995, 251(1): 15–26. DOI: 10.1016/0921-4534(95)00398-3

[12] Li Y X, Ta W R, Gao Y W, et al. Transport current distribution on Nb 3 Sn strand for TARSIS. Physica C: Superconductivity, 2013, 489: 25–31. DOI: 10.1016/j.physc.2013.03.052

[13] Bean C P. Magnetization of hard superconductors. Physical Review Letters, 1962, 8(6): 250. DOI: 10.1103/PhysRevLett.8.250

[14] Kim Y, Hempstead C, Strnad A. Magnetization and critical supercurrents. Physical Review, 1963, 129(2): 528. DOI: 10.1103/PhysRev.129.528

[15] Hong Z Y, Campbell A M, Coombs T A. Numerical solution of critical state in superconductivity by finite element software. Superconductor Science and Technology, 2006, 19(12): 1246. DOI: 10.1088/0953-2048/19/12/004

[16] Ikuta H, Hirota N, Nakayama Y, et al. Giant magnetostriction in Bi2Sr2CaCu2O8 single crystal in the superconducting state and its mechanism. Physical Review Letters, 1993, 70(14): 2166. DOI: 10.1103/PhysRevLett.70.2166

[17] Ikuta H, Kishio K, Kitazawa K. Critical state models for flux-pinning-induced magnetostriction in type-II superconductors. Journal of Applied Physics, 1994, 76(8): 4776–4786. DOI: 10.1063/1.357249

[18] Johansen T H. Flux-pinning-induced stress and strain in superconductors: Case of a long circular cylinder. Physical Review B, 1999, 60(13): 9690. DOI: 10.1103/PhysRevB.60.9690

[19] Johansen T H. Flux-pinning-induced stress and strain in superconductors: Long rectangular slab. Physical Review B, 1999, 59(17): 11187. DOI: 10.1103/PhysRevB.59.11187

[20] Johansen T H, Shantsev D V. Magnetostrictive behaviour of thin superconducting disks. Superconductor Science and Technology, 2003, 16(9): 1109. DOI: 10.1088/0953-2048/16/9/324

[21] Eremenko V, Sirenko V, Szymczak H, et al. Magnetostriction of thin flat superconductor in a transverse magnetic field. Superlattices and Microstructures, 1998, 24(3): 221–226. DOI: 10.1006/spmi.1998.0583

[22] Nabiałek A, Szymczak H, Sirenko V, et al. Influence of the real shape of a sample on the pinning induced magnetostriction. Journal of Applied Physics, 1998, 84(7): 3770–3775. DOI: 10.1063/1.368555

[23] Çelebi S, Inanir F, LeBlanc M. Coexistence of critical and normal state magnetostrictions in type II superconductors: a model exploration. Journal of Applied Physics, 2007, 101(1): 3906. DOI: 10.1063/1.2407266

[24] Xue F, Yong H D, Zhou Y H. Effect of flux creep and viscous flux flow on flux-pinning-induced stress and magnetostriction in a long rectangular slab superconductor. Journal of Applied Physics, 2010, 108(10): 103910. DOI: 10.1063/1.3506704

[25] Huang C G, Yong H D, Zhou Y H. Magnetostrictive behaviors of type-II superconducting cylinders and rings with finite thickness. Superconductor Science and Technology, 2013, 26(10): 105007. DOI: 10.1088/0953-2048/26/10/105007

[26] Xue C, He A, Yong H, et al. Magneto-elastic behaviour of thin type-II superconducting strip with field-dependent critical current. Journal of Applied Physics, 2013, 113(2): 023901. DOI: 10.1063/1.4773483

[27] Yong H D, Zhou Y H. Flux pinning induced stress and magnetostriction in a long elliptic cylindrical superconductor. Journal of Applied Physics, 2013, 114(2): 023902. DOI: 10.1063/1.4811531

[28] Huang C G, Zhou Y H. Magnetic and magnetostrictive properties of finite superconducting cylinders containing a cavity. Journal of Applied Physics, 2014, 115(3): 033904. DOI: 10.1063/1.4862856

[29] Yang Y, Xiao L-Y, Li X-H. Impact of viscous flux flow on the stress in long rectangular slab superconductors. Journal of Applied Physics, 2010, 107(2): 3910. DOI: 10.1063/1.3284080

[30] Johansen T H. Flux-pinning-induced stress and magnetostriction in bulk superconductors. Superconductor Science and Technology, 2000, 13(10): R121. DOI: 10.1088/0953-2048/13/10/201

[31] Johansen T, Wang C, Chen Q, et al. Enhancement of tensile stress near a hole in superconducting trapped-field magnets. Journal of Applied Physics, 2000, 88(5): 2730–2733. DOI: 10.1063/1.1287123

[32] Yong H D, Zhou Y H. Stress distribution in a flat superconducting strip with transport current. Journal of Applied Physics, 2011, 109(7): 073902. DOI: 10.1063/1.3561366

[33] Yang Y, Wang X. Magnetization and magnetoelastic behavior of a functionally graded rectangular superconductor slab. Journal of Applied Physics, 2014, 116(2): 023901. DOI: 10.1063/1.4887138

[34] Yang Y, Wang X. Stress and magnetostriction in an infinite hollow superconducting cylinder with a filling in its central hole. Physica C: Superconductivity, 2013, 485: 58–63. DOI: 10.1016/j.physc.2012.10.003

[35] Feng W J, Han X, Ma P. Flux-pinning-induced stress and magnetostriction in a functionally graded long rectangular superconductor slab. Journal of Applied Physics, 2011, 110(6): 063917. DOI: 10.1063/1.3639302

[36] Yong H D, Zhou Y H. Effect of nonsuperconducting particles on the effective magnetostriction of bulk superconductors. Journal of Applied Physics, 2008, 104(4): 043907. DOI: 10.1063/1.2952042

[37] Yong H D, Yang Y, Zhou Y H. Mechanical behaviours in Bi2223/Ag/Ag alloy composite tape with different volume fractions. Journal of Superconductivity and Novel Magnetism, 2016, 29(2): 329–336. DOI: 10.1007/s10948-015-3358-1

[38] Tomita M, Murakami M. High-temperature superconductor bulk magnets that can trap magnetic fields of over 17 tesla at 29 K. Nature, 2003, 421(6922): 517–520. DOI: 10.1038/nature01350

[39] Zeng J, Yong H D, Zhou Y H. Edge-crack problem in a long cylindrical superconductor. Journal of Applied Physics, 2011, 109(9): 093920. DOI: 10.1063/1.3585830

[40] Zeng J, Zhou Y H, Yong H D. Fracture behaviors induced by electromagnetic force in a long cylindrical superconductor. Journal of Applied Physics, 2010, 108(3): 033901. DOI: 10.1063/1.3456038

[41] Zhou Y H, Yong H D. Crack problem for a long rectangular slab of superconductor under an electromagnetic force. Physical Review B, 2007, 76(9): DOI: 10.1103/PhysRevB.76.094523

[42] Yong H D, Jing Z, Zhou Y H. Crack problem for superconducting strip with finite thickness. International Journal of Solids and Structures, 2014, 51(3): 886–893. DOI: 10.1016/j.ijsolstr.2013.11.013

[43] Yong H D, Xue C, Zhou Y H. Thickness dependence of fracture behaviour in a superconducting strip. Superconductor Science and Technology, 2013, 26(5): 055003. DOI: 10.1088/0953-2048/26/5/055003

[44] Yong H D, Zhou Y H. Crack problem for thin superconducting strip in a perpendicular magnetic field. IEEE Transactions on Applied Superconductivity, 2012, 22(2): 8400905. DOI: 10.1109/TASC.2011.2178093

[45] Gao S W, Feng W J, Liu J X. Fracture problems of a superconducting slab with a central kinked crack. Journal of Applied Physics, 2013, 114(24): 243907. DOI: 10.1063/1.4852495

[46] Gao Z W, Zhou Y H. Crack growth for a long rectangular slab of superconducting trapped-field magnets. Superconductor Science and Technology, 2008, 21(9): 095010. DOI: 10.1088/0953-2048/21/9/095010

[47] Wang X, Yong H D, Xue C, et al. Inclined crack problem in a rectangular slab of superconductor under an electromagnetic force. Journal of Applied Physics, 2013, 114(8): 083901. DOI: 10.1063/1.4818284

[48] Xue C, He A, Zhou Y H. Fracture problem of the thin superconducting strip with transverse crack, In: 13th International Conference on Fracture, Beijing, China, 2013. p. 1–9.

[49] Gao Z W, Zhou Y H, Lee K Y. The interaction of two collinear cracks in a rectangular superconductor slab under an electromagnetic force. Physica C: Superconductivity, 2010, 470(15): 654–658. DOI: 10.1016/j.physc.2010.06.008

[50] Gao Z W, Zhou Y H, Lee K Y. Crack-inclusion problem for a long rectangular slab of superconductor under an electromagnetic force. Computational Materials Science, 2010, 50(2): 279–282. DOI: 10.1016/j.commatsci.2010.08.015

[51] Xue F, Gou X F. Crack problem for a bulk superconductor with nonsuperconducting inclusions under an electromagnetic force. AIP Advances, 2015, 5(4): 047128. DOI: 10.1063/1.4918752

[52] Xue F, Zhang Z X, Gou X F. Fracture behavior of an inclined crack interacting with a circular inclusion in a high-TC superconductor under an electromagnetic force. AIP Advances, 2015, 5(11): 117141. DOI: 10.1063/1.4936422

[53] Feng W J, Zhang R, Ding H M. Crack problem for an inhomogeneous orthotropic superconducting slab under an electromagnetic force. Physica C: Superconductivity, 2012, 477: 32–35. DOI: 10.1016/j.physc.2012.02.027

[54] Feng W J, Liu Q F, Han X. Crack problem for a functionally graded thin superconducting film with field dependent critical currents. Mechanics Research Communications, 2014, 61: 36–40. DOI: 10.1016/j.mechrescom.2014.07.005

[55] Feng W J, Liu Q F, Su R. Fracture behaviors of a functionally graded thin superconducting film with transport currents based on the strain energy density theory. Theoretical and Applied Fracture Mechanics, 2014, 74: 73–78. DOI: 10.1016/j.tafmec.2014.07.002

[56] Yan Z, Gao S W, Feng W J. Fracture problem for an external circumferential crack in a functionally graded superconducting cylinder subjected to a parallel magnetic field. Physica C: Superconductivity and its Applications, 2015, 521–522: 5–12. DOI: 10.1016/j.physc.2015.12.003

[57] Gao Z, Zheng Z Y, Li X Y. Fracture problem of a nonhomogeneous high temperature superconductor slab based on real fundamental solutions. Physica C: Superconductivity and its Applications, 2015, 519: 5–12.

[58] Gao Z W, Zhou Y H. Dynamic stress intensity factors of mode-I crack in high temperature superconductor. Physica C: Superconductivity, 2013, 495: 169–173. DOI: 10.1016/j.physc.2013.09.013

[59] Patel A, Filar K, Nizhankovskii V I, et al. Trapped fields greater than 7 T in a 12 mm square stack of commercial high-temperature superconducting tape. Applied Physics Letters, 2013, 102(10): 102601. DOI: 10.1063/1.4795016

[60] Freund L. Substrate curvature due to thin film mismatch strain in the nonlinear deformation range. Journal of the Mechanics and Physics of Solids, 2000, 48(6): 1159–1174. DOI: 10.1016/S0022-5096(99)00070-8

[61] Olsson E, Gupta A, Thouless M D, et al. Crack formation in epitaxial [1 1 0] thin films of $YBa_2Cu_3O_{7-\delta}$ and $PrBa_2Cu_3O_{7-x}$ on [1 1 0]$SrTiO_3$ substrates. Applied Physics Letters, 1991, 58(15): 1682. DOI: 10.1063/1.105110

[62] Yong H D, Zhou Y H. Interface crack between superconducting film and substrate. Journal of Applied Physics, 2011, 110(6): 063924. DOI: 10.1063/1.3634019

[63] Jing Z, Yong H D, Zhou Y H. Flux-pinning-induced interfacial shearing and transverse normal stress in a superconducting coated conductor long strip. Journal of Applied Physics, 2012, 112(4): 043908. DOI: 10.1063/1.4748338

[64] Jing Z, Yong H D, Zhou Y H. Shear and transverse stress in a thin superconducting layer in simplified coated conductor architecture with a pre-existing detachment. Journal of Applied Physics, 2013, 114(3): 033907. DOI: 10.1063/1.4813869

[65] Valvo P S. A revised virtual crack closure technique for physically consistent fracture mode partitioning. International Journal of Fracture, 2012, 173(1): 1–20. DOI: 10.1007/s10704-011-9658-y

[66] Rybicki E F, Kanninen M F. A finite element calculation of stress intensity factors by a modified crack closure integral. Engineering Fracture Mechanics, 1977, 9(4): 931–938. DOI: 10.1016/0013-7944(77)90013-3

[67] Irwin G R. Onset of fast crack propagation in high strength steel and aluminum, In: Sagamore research conference proceedings, 1956. p. 289–305.

[68] Yu H J. Investigations on fracture mechanics of nonhomogeneous materials with complex interfaces [thesis]. Harbin Institute of technology; 2010.

[69] Yu H J, Wu L Z, Guo L C, et al. Interaction integral method for the interfacial fracture problems of two nonhomogeneous materials. Mechanics of Materials, 2010, 42(4): 435–450. DOI: 10.1016/j.mechmat.2010.01.001

[70] Nagashima T, Omoto Y, Tani S. Stress intensity factor analysis of interface cracks using X-FEM. International Journal for Numerical Methods in Engineering, 2003, 56(8): 1151–1173. DOI: 10.1002/nme.604

[71] Miyazaki N, Ikeda T, Soda T, et al. Stress intensity factor analysis of interface crack using boundary element method. JSME International Journal, 1993, 36(1): 36–42. DOI: 10.1016/0013-7944(93)90266-U

[72] Suo Z G, Hutchinson J W. Interface crack between two elastic layers. International Journal of Fracture, 1990, 43(1): 1–18. DOI: 10.1007/BF00018123

[73] Dundurs J. Mathematical Theory of Dislocations. New York: American Society of Mechanical Engineering, 1969: 70.

[74] Dizon J R C, Gorospe A B, Shin H S. Numerical analysis of stress distribution in Cu-stabilized GdBCO CC tapes during anvil tests for the evaluation of transverse delamination strength. Superconductor Science and Technology, 2014, 27(5): 055023. DOI: 10.1088/0953-2048/27/5/055023

[75] Prigozhin L. The Bean model in superconductivity: Variational formulation and numerical solution. Journal of Computational Physics, 1996, 129(243): 190–200. DOI: 10.1006/jcph.1996.0243

IntechOpen